

SLAC-PUB-5400  
DESY-91-051  
May 1991  
(T/E)

## Measurement of the Direct Photon Spectrum from $\Upsilon(1S)$ Decays

The Crystal Ball Collaboration

A. Bizzi<sup>1</sup>, J. Schütte<sup>2</sup>, D. Antreayan<sup>3</sup>, Ch. Biedler<sup>4</sup>, J.K. Bienlein<sup>1</sup>, E.D. Bloom<sup>10</sup>,  
I. Brock<sup>2</sup>, K. Brockmüller<sup>4</sup>, A. Cartacci<sup>6</sup>, M. Cavalli-Sforza<sup>1</sup>, A. Compagnucci<sup>6</sup>,  
G. Conforto<sup>6</sup>, S. Cooper<sup>9,a</sup>, D. Coyne<sup>1</sup>, K.H. Fairfield<sup>10</sup>, G. Folger<sup>5</sup>, A. Fridman<sup>10</sup>,  
G. Glaser<sup>5</sup>, G. Godfrey<sup>10</sup>, K. Graal<sup>7</sup>, F.H. Heimlich<sup>5,6</sup>, F.H. Heinsius<sup>7</sup>,  
R. Hofstadter<sup>8,b</sup>, J. Inoué<sup>8</sup>, Z. Jakubowski<sup>3</sup>, H. Janssen<sup>9</sup>, K. Karch<sup>3,10</sup>, S. Kehl<sup>11</sup>,  
T. Kiel<sup>7</sup>, H. Kilian<sup>11</sup>, I. Kirkbride<sup>10</sup>, M. Kobel<sup>5</sup>, W. Koch<sup>4</sup>, A.C. König<sup>9</sup>,  
K. Königsman<sup>10,c</sup>, S. Krüger<sup>7</sup>, G. Landi<sup>6</sup>, R. Lekebusch<sup>7</sup>, S. Lowe<sup>10</sup>, B. Lutz<sup>5</sup>,  
H. Marsiske<sup>3,9</sup>, W. Maschmann<sup>7</sup>, P. McBride<sup>8</sup>, W.J. Metzger<sup>9</sup>, B. Monteleoni<sup>6</sup>,  
B. Muryn<sup>2,d</sup>, B. Niczyporuk<sup>10</sup>, G. Nowak<sup>3</sup>, P.G. Pefter<sup>6</sup>, M. Reidenbach<sup>9</sup>,  
M. Scheer<sup>11</sup>, P. Schmitt<sup>11</sup>, J. Scholtanus<sup>9</sup>, D. Stevers<sup>7</sup>, T. Skwarnicki<sup>1</sup>, V. Stock<sup>7</sup>,  
K. Strauch<sup>6</sup>, U. Strobbusch<sup>7</sup>, J. Tompkins<sup>10</sup>, B. van Uiterl<sup>10</sup>, R.T. Van de Walle<sup>9</sup>,  
A. Voigt<sup>4</sup>, U. Volland<sup>5</sup>, K. Wachs<sup>1</sup>, H. Wegener<sup>5</sup>, D.A. Williams<sup>1,7</sup>

<sup>1</sup> University of California at Santa Cruz, Santa Cruz, CA 95064, USA

<sup>2</sup> Carnegie-Mellon University<sup>1</sup>, Pittsburgh, PA 15213, USA

<sup>3</sup> Cracow Institute of Nuclear Physics, PL-30055 Cracow, Poland

<sup>4</sup> Deutsches Elektronen Synchrotron DESY, D-2000 Hamburg, Germany

<sup>5</sup> Università Erlangen-Nürnberg<sup>9</sup>, D-8520 Erlangen, Germany

<sup>6</sup> INFN and University of Firenze, I-50125 Firenze, Italy

<sup>7</sup> Universität Hamburg, I. Institut für Experimentalphysik<sup>h</sup>, D-2000 Hamburg, Germany

<sup>8</sup> Harvard University<sup>i</sup>, Cambridge, MA 02138, USA

<sup>9</sup> University of Nijmegen and NIKHEF<sup>k</sup>, NL-6525 ED Nijmegen, The Netherlands

<sup>10</sup> Department of Physics<sup>l</sup>, HEPL, and Stanford Linear Accelerator Center<sup>m</sup>,  
Stanford University, Stanford, CA 94305, USA

<sup>11</sup> Universität Würzburg<sup>n</sup>, D-8700 Würzburg, Germany

## Abstract

Using the Crystal Ball detector at the  $e^+e^-$  storage ring DORIS II, we have measured the energy spectrum of direct photons from  $\Upsilon(1S)$  decays. According to QCD, these photons result from the decays of the  $\Upsilon(1S)$  resonance into one photon and two gluons,  $\Upsilon(1S) \rightarrow \gamma gg \rightarrow \gamma + hadrons$ . The shape of our spectrum does not agree with that calculated in lowest order QCD, but can be described well by a prediction incorporating gluon self-interaction. Using this fit, the ratio  $R_\gamma = \Gamma(\Upsilon \rightarrow \gamma gg) / \Gamma(\Upsilon \rightarrow ggg)$  is determined to be  $(2.7 \pm 0.2 \pm 0.1)\%$ . From this ratio we deduce the strong coupling constant in the  $\overline{MS}$  scheme at  $Q^2 = 2.2 \text{ GeV}^2$  and find  $\alpha_s = 0.25 \pm 0.02 \pm 0.01$ .

(Submitted to Zeitschrift für Physik C)

<sup>a)</sup> Present Address: Max-Planck-Institut für Physik, D-8000 München 40, Germany

<sup>b)</sup> Deceased

<sup>c)</sup> Present Address: CERN, CH-1211 Genève 23, Switzerland

<sup>d)</sup> Permanent Address: Institute of Physics and Nuclear Techniques, AGH, PL-30056 Cracow, Poland

<sup>e)</sup> Supported by the National Science Foundation, grant No. PHY85-12115

<sup>f)</sup> Supported by the U.S. Department of Energy, contract No. DE-AC02-76ER03066

<sup>g)</sup> Supported by the German Bundesministerium für Forschung und Technologie, contract No. 051 ER 12P

<sup>h)</sup> Supported by the German Bundesministerium für Forschung und Technologie, contract No. 051 III 111(7) and by the Deutsche Forschungsgemeinschaft

<sup>i)</sup> Supported by the U.S. Department of Energy, contract No. DE-AC02-76ER03064

<sup>j)</sup> Supported by Stichting voor Fundamenteel Onderzoek der Materie - Nederlandse Organisatie voor Wetenschappelijk Onderzoek (FOM-ZWO)

<sup>k)</sup> Supported by the U.S. Department of Energy, contract No. DE-AC03-76SF00326

<sup>l)</sup> Supported by the U.S. Department of Energy, grant No. PHY81-07395

<sup>m)</sup> Supported by the U.S. Department of Energy, contract No. DE-AC03-76SF00615

<sup>n)</sup> Supported by the German Bundesministerium für Forschung und Technologie, contract No. 051 IVU 111(1)

## Introduction

According to the QCD theory of strong interactions, the  $\Upsilon(1S)$  decays predominantly into hadrons via a three-gluon intermediate state [1]. The decay into one photon and two gluons is also allowed [2], but is suppressed by a factor  $\mathcal{O}(\alpha_{em}/\alpha_s)$  compared to the dominant decay, where  $\alpha_{em}$  and  $\alpha_s$  are the electromagnetic and the strong coupling constants, respectively.

A perturbative QCD calculation in next-to-leading order in  $\alpha_s$  gives for the ratio  $R_\gamma$  of the partial decay widths [3]

$$R_\gamma = \frac{\Gamma(\Upsilon \rightarrow \gamma g g)}{\Gamma(\Upsilon \rightarrow g g g)} = \frac{36}{5} \frac{\alpha_{em}}{\alpha_s} \left(\frac{e_b}{e}\right)^2 \left[1 + (2.2 \pm 0.6) \frac{\alpha_s}{\pi}\right], \quad (1)$$

where  $e_b = -\frac{1}{3}e$  is the electric charge of the  $b$ -quark and the  $\overline{\text{MS}}$  renormalization scheme at  $Q^2 = (0.157 M_\Upsilon)^2 = 2.2 \text{ GeV}^2$  is used. The large QCD corrections affecting the  $\gamma g g$  and  $g g g$  decay widths nearly cancel in this ratio, so that a measurement of  $R_\gamma$  should allow a reliable determination of  $\alpha_s$ .

In addition, the shape of the direct photon spectrum contains information on the non-abelian structure of QCD. In fact, the lowest order perturbative calculation predicts [2] an almost linearly rising spectrum in  $z = E_\gamma/E_{B\text{-beam}}$  with a sharp decrease at  $z = 1$ , in analogy to the decay of ortho-positronium [4]. A summation of leading logarithmic contributions to all orders in perturbation theory performed by Photradis [5] yields a slight softening of the spectrum compared to [2]. This spectrum, however, is still quite similar to that obtained by lowest order QCD and peaks close to  $z = 1$ .

A calculation by Field [6] predicts a much softer spectrum using a parton-shower Monte Carlo approximation to perturbative QCD that estimates the effect of the self-coupling of gluons. The two gluons recoiling against the direct photon acquire a non-zero invariant mass by radiating further bremsstrahlung gluons. This leads to a suppression of direct photons with energies close to the beam energy, yielding a spectrum with a maximum at  $z \approx 0.7$ .

## Data sample and detector

The data used for this analysis were collected with the Crystal Ball detector at the  $e^+e^-$  storage ring DORIS II and represent an integrated luminosity of  $17.1 \pm 0.4 \text{ pb}^{-1}$  taken on the  $\Upsilon(1S)$  resonance, corresponding to  $153.5 \times 10^3$  observed  $\Upsilon(1S)$  decays, and  $19.2 \pm 0.5 \text{ pb}^{-1}$  taken in the continuum.

The Crystal Ball detector, described in detail elsewhere [7], is a nonmagnetic calorimeter designed to measure precisely the energies and directions of electromagnetically showering particles. Its main part (the Ball) is a spherical shell, consisting of 672 optically isolated NaI(Tl) crystals. The Ball covers 93% of the entire solid angle, two holes being left for the beam pipe. Each crystal has the shape of a truncated triangular pyramid pointing to the  $e^+e^-$  interaction region and projects a radial distance of 16 radiation lengths (corresponding to about one nuclear interaction length).

Showers produced by high energy ( $> 1 \text{ GeV}$ ) electrons and photons in the Ball deposit about 94% of their energy in 13 adjacent crystals in an almost symmetric

pattern, resulting in an energy resolution  $\sigma_E/E = (2.7 \pm 0.2)\% \sqrt{E/\text{GeV}}$  and an angular resolution of about  $2^\circ$ .

Muons and charged hadrons that do not undergo a strong interaction deposit energy by ionization only. Minimum ionizing particles deposit typically 200 MeV in one or two crystals. If an energetic hadron interacts strongly while traversing the Ball, the deposited energy is in general much larger than 200 MeV and the pattern of the hadronic shower is quite irregular compared to that of an electromagnetic shower. The directions of charged particles emerging from the  $e^+e^-$  interaction region are measured by a set of proportional wire chambers located inside the Ball. The chambers consist of 800 aluminum tubes, assembled in 4 cylindrical double-layers around the beam pipe.

## Event and Photon Selection

The selection of  $\gamma g g$  events is designed to suppress background from QED processes, cosmic rays, beam-gas and beam-wall interactions. We require a total energy deposited in the Ball  $E_{\text{Ball}} > 0.3 E_{\text{CMS}}$ , where  $E_{\text{CMS}} = 2 E_{p\text{-beam}} (= 9.46 \text{ GeV})$  on the  $\Upsilon(1S)$  resonance). We also require a minimum transverse energy  $E_{T\text{-min}} = \sum_i E_i \sin \theta_i > 0.25 E_{\text{CMS}}$ , where we sum over all crystals; here  $E_i$  is the energy deposited in the  $i^{\text{th}}$  crystal and  $\theta_i$  is the angle between the beam axis and the center of that crystal. These cuts mainly reject beam-related background events, which deposit most of their energy at small angles with respect to the beam axis.

Background events from the QED processes  $e^+e^- \rightarrow e^+e^-(\gamma)$  and  $e^+e^- \rightarrow \gamma\gamma(\gamma)$  generally contain two high energy particles depositing almost their entire energy in the Ball. In contrast, it is very unlikely in  $\gamma g g$  events that a particle other than the direct photon deposit a large amount of energy in the Ball, since the two gluons fragment into several hadrons, most of which deposit only part of their energy. We therefore require a multiplicity  $N_{\text{particles}} \geq 3$  and an energy deposited by the second most energetic particle to be less than  $0.65 E_{\text{CMS}} - 0.5 E_{\text{Ball}}$ . These cuts reject almost all QED background events, while maintaining a high efficiency for  $\gamma g g$  events up to the highest  $\gamma$  energies. The small QED background still left after this selection is subtracted at a later stage of the analysis using continuum data.

Photon candidates are selected from energy clusters in the calorimeter by requiring  $z = E_\gamma/E_{\text{beam}} > 0.3$ , a direction within the geometrical acceptance of the tube chambers ( $|\cos \theta| < 0.80$ ), no tube chamber track associated with the cluster direction, and a lateral energy distribution consistent with that expected for a single electromagnetically showering particle. The last cut is chosen rather loose as the lateral energy distribution of the photon candidates will be used to discriminate the  $\pi^0$  background in a later stage; it is, however, effective in removing interacting hadrons and most of the overlapping showers. The resulting spectrum of photon candidates is shown in Fig. 1 as the solid histogram.

The efficiency of the event and photon selection is determined using  $\gamma g g$  Monte Carlo events produced with the Lund 6.3 generator [8]. The generated events are passed through a complete detector simulation, which uses the EGS 3 program [9] for electrons and photons and the GHEISHA 6 program [10] for hadronic interactions. The Monte Carlo events are then analyzed exactly like the real data. The efficiency,

shown in Fig. 2, is smooth and rather flat with values of at least 50% in the range  $0.35 < z < 1$ .

## Background Subtraction

The background due to continuum processes ( $e^+e^- \rightarrow q\bar{q}(\gamma)$ ) and remaining QED events) is determined from data taken in the nearby continuum, which are analyzed exactly like the on-resonance data. The continuum data, scaled by the luminosity ratio and corrected for the energy dependence of the continuum cross section, are shown in Fig. 1 as the dotted histogram. This continuum spectrum is then subtracted from the on-resonance spectrum of photon candidates.

The background remaining after the continuum subtraction is mainly due to high energy  $\pi^0$ 's where the two decay photons are so close to each other that the showers overlap and appear as a single energy cluster in the calorimeter ('merged'  $\pi^0$ 's). Two methods are used to correct for this background, which dominates the spectrum for  $z < 0.5$  (solid points in Fig. 1): a statistical analysis of the shower shape (method 1) and a Monte Carlo calculation of the background (method 2). Note that previous investigations [11, 12, 13] of the direct photon spectrum have essentially followed the second approach; thus our first method provides an independent check on the shape of the photon spectrum.

### Statistical Analysis of Shower Shape (Method 1)

This method [14] utilizes the different distributions of the squared angular width  $\Theta^2$  of the lateral energy distribution of photon and merged  $\pi^0$  showers [15]. In order to calculate the second moment  $\Theta^2$ , we first determine the center of gravity  $\vec{c}$  of the shower from  $\vec{c} = (1/E) \sum_i \vec{n}_i E_i$ , where the sum includes all crystals of the shower.  $E$  denotes the total shower energy,  $E_i$  is the energy in the  $i^{\text{th}}$  crystal and  $\vec{n}_i$  is the unit vector pointing to its center. The value of  $\Theta^2$  is then calculated with  $\Theta^2 = (1/E) \sum_i (\vec{c} - \vec{n}_i)^2 E_i$ , where the sum again is over all crystals of the shower.

The lateral shower extension of a high energy  $\pi^0$  is on average larger than the corresponding value for a single photon of the same energy. Since the two photons from a  $\pi^0$  come closer with increasing  $\pi^0$  energy, the reliability of a statistical differentiation between photons and  $\pi^0$ 's is energy dependent: while the average ( $\Theta^2$ ) value for  $\pi^0$ 's is about twice as large as that for photons at  $E = 2$  GeV, the difference shrinks to about 20% at  $E = 5$  GeV. For each  $z$  bin ( $\Delta z = 0.05$ ), the  $\Theta^2$  distribution for on-resonance data is calculated, and the corresponding distribution for continuum data is subtracted. Due to the sensitivity of this method to the absolute  $\pi^0$  energy, only that part ( $7.9 \text{ pb}^{-1}$ ) of the continuum data, which was taken just below the  $\Upsilon(1S)$  resonance, is used for this subtraction.

The resulting  $\Theta^2$  distributions for  $\Upsilon(1S)$  decays are then fitted with Monte Carlo  $\Theta^2$  distributions for photons and merged pions. The expected distributions for direct  $\gamma$ 's have been extracted using photons in Monte Carlo  $\gamma\gamma\gamma$  events, whereas those for  $\pi^0$ 's have been obtained by analyzing neutral shower depositions in Monte Carlo three-gluon and  $q\bar{q}$  events. All Monte Carlo events have been passed through the complete detector simulation described above. Note that the  $\Theta^2$  distributions for  $\pi^0$ 's

from Monte Carlo and data also contain small contributions from accidental overlap of energy depositions and from single photons from well-separated  $\pi^0$  decays; the latter contribute a tail towards small values of  $\Theta^2$ . Thus separated  $\pi^0$  decays are also included in this analysis.

The fit result for the  $\Theta^2$  distribution of photon candidates with scaled energies between  $z = 0.60$  and  $0.65$  is shown in Fig. 3. By repeating this fitting procedure for all energy bins, we can split the continuum-subtracted spectrum of photon candidates on a statistical basis into a photon spectrum and a  $\pi^0$  background spectrum. To minimize the effect of statistical fluctuations, we fit the  $\pi^0$  spectrum with an exponential function, shown as the solid curve in Fig. 1, and subtract the fit result from the spectrum of photon candidates to get the photon spectrum. After correcting for the efficiency, we obtain the final photon spectrum shown in Fig. 4. This method is effective in the region  $z \geq 0.35$ ; at lower energies the background of well-separated photons from  $\pi^0$  decays prevents a good measurement of the number of direct photons.

### Monte Carlo Calculation (Method 2)

In this analysis [16] the background from other  $\Upsilon(1S)$  decays is estimated by modelling the decays  $\Upsilon(1S) \rightarrow ggg \rightarrow hadrons$  and  $\Upsilon(1S) \rightarrow q\bar{q} \rightarrow hadrons$  with the Lund generator [8], and  $\Upsilon(1S) \rightarrow \tau^+\tau^-$  decays with a QED generator [17]. Detector response is again simulated as for the Monte Carlo events discussed above. In this analysis we use harder cuts on the lateral shape of the shower of photon candidates. This suppresses the  $\pi^0$  background by about an order of magnitude, thus decreasing our reliance on the Monte Carlo estimate, but also reducing our efficiency for direct photons by about 40%.

The energy spectrum of photon candidates from Monte Carlo events is scaled to the appropriate luminosity and, together with the continuum spectrum, is subtracted from the on-resonance spectrum of photon candidates. The resulting direct photon spectrum, corrected for efficiency, is shown in Fig. 5. This method is effective in the region  $z \geq 0.50$ , where we are not very sensitive to the evaluation of the Monte Carlo  $\pi^0$  background.

## Results and Conclusions

The two direct photon spectra obtained above agree well with each other with a confidence level (CL) of 58%. The spectra are compared to the predictions from lowest order QCD [2], Photiadis' model [5] and Field's model [6]. Fits with free overall normalization yield the  $\chi^2$  values given in Table 1. Both spectra are in good agreement with Field's model with CLs of 61% and 91% for the spectra from Method 1 and 2, respectively. The hard spectrum predicted by lowest order QCD is clearly ruled out (CL  $< 1.4 \times 10^{-4}$  for both spectra), as can be seen in Figures 4 and 5. The fits to Photiadis' model yield CLs of 0.9% and 0.14%, respectively. We conclude that Field's model is strongly preferred over that of Photiadis.

We use Field's prediction to extrapolate the spectra to  $z = 0$  and obtain the number of direct photons stated in Table 1, where the first error is statistical and the second is systematic. The systematic error for the first method is estimated by

repeating the complete analysis with varied selection cuts, shifted Monte Carlo  $\Theta^2$  distributions, and altered fit ranges in  $\Theta^2$  [14]. For the second method the dominant systematic error results from the subtraction of the  $\pi^0$  background modelled by Monte Carlo. We determined the error [16] by varying the photon selection cuts and modifying Monte Carlo parameters (e.g., the  $p_T$  of the gluon jets). For both methods smaller contributions are included due to the omission of final state bremsstrahlung from the process  $\Upsilon(1S) \rightarrow \gamma q\bar{q} \rightarrow \gamma + \text{hadrons}$  [14, 18], and the uncertainty in the extrapolation of the photon spectra to  $z = 0$ .

Table 1: Results of fits of the two photon spectra to theoretical models.

Fit Model	Lo. QCD [2]	Pluriadis [5]	Field [6]	Field [6]	
Fit Range	$\chi^2/\text{dof}$	$\chi^2/\text{dof}$	$\chi^2/\text{dof}$	$N_\gamma(10^3)$	
Method 1	$z > 0.35$	40/13	28/13	11/13	$3.7 \pm 0.3^{+0.5}_{-0.4}$
Method 2	$z > 0.50$	41/9	27/9	4/9	$4.3 \pm 0.3^{+0.4}_{-0.5}$

We combine the results from both methods and obtain for the total number of photons  $N_\gamma = (4.0 \pm 0.3 \pm 0.5) \times 10^3$ . Correcting the number of observed hadronic  $\Upsilon$  decays for hadronic efficiencies and subtracting the contribution of  $\Upsilon \rightarrow q\bar{q}, \tau^+\tau^-, \gamma g g$  decays, we obtain for the number of  $\Upsilon \rightarrow g g g$  decays [14]  $N_{ggg} = (1.47 \pm 1 \pm 6) \times 10^3$  and therefore a ratio  $R_\gamma = N_\gamma/N_{ggg} = (2.7 \pm 0.2 \pm 0.4)\%$ . Inserting  $R_\gamma$  in (1) yields for the strong coupling constant in the  $\overline{\text{MS}}$  renormalization scheme at  $Q^2 = 2.2 \text{ GeV}^2$  a value  $\alpha_s = 0.25 \pm 0.02 \pm 0.04$ .

The results of this analysis are compared to those obtained by previous experiments in Table 2. The shape of our spectrum is consistent with those of ARGUS [11] and CLEO [12], but in disagreement with that measured by CUSB [13]. Our spectrum confirms with better energy resolution ARGUS' result that lowest order QCD does not describe the experimental photon spectrum. Our values of  $R_\gamma$  and  $\alpha_s(2.2 \text{ GeV}^2)$  are also consistent with the results from the other experiments. Excluding the CUSB measurement, we obtain an average of  $R_\gamma = (2.77 \pm 0.15)\%$  and  $\alpha_s(2.2 \text{ GeV}^2) = 0.24 \pm 0.02$ , where the errors include the statistical and systematic errors.

Table 2: Comparison with other experiments. The energy resolutions of the respective calorimeters are given for a photon energy of 4.5 GeV.

Experiment	$\sigma_E/E$	Shape	$R_\gamma$ (%)	$\alpha_s(2.2 \text{ GeV}^2)$
CUSB [13]	3%	Hard [2, 5]	$2.99 \pm 0.59$	$0.226^{+0.087}_{-0.012}$
CLEO [12]	10%	[6] assumed	$2.54 \pm 0.18 \pm 0.14$	$0.27^{+0.03+0.03}_{-0.02-0.02}$
ARGUS [11]	8%	Soft [6]	$3.00 \pm 0.13 \pm 0.18$	$0.225 \pm 0.011 \pm 0.019$
This measurement	2%	Soft [6]	$2.7 \pm 0.2 \pm 0.4$	$0.25 \pm 0.02 \pm 0.04$

In conclusion, a new analysis of the direct photon energy spectrum from  $\Upsilon(1S)$  decays by the Crystal Ball experiment rules out the hard spectra predicted by lowest order QCD, but is in good agreement with the softer spectrum predicted by Field, who includes an estimate of the self-coupling of gluons. This suggests substantial

contributions by higher order QCD corrections. Our value of  $R_\gamma = (2.7 \pm 0.2 \pm 0.4)\%$  results in  $\alpha_s(2.2 \text{ GeV}^2) = 0.25 \pm 0.02 \pm 0.04$ . This value of  $\alpha_s$  is consistent with the results of other  $\alpha_s$  measurements at higher  $Q^2$  values [19, 20].

## Acknowledgments

We would like to thank the DESY and SLAC directorates for their support. This experiment would not have been possible without the dedication of the DORIS machine group as well as the experimental support groups at DESY. The visiting groups thank the DESY laboratory for the hospitality extended to them. Z.J., B.N., and G.N. thank DESY for financial support. E.D.B., R.H., and K.S. have benefited from financial support from the Humboldt Foundation. K. Königsmann acknowledges support from the Heisenberg Foundation.

## References

- [1] T. Appelquist, H.D. Politzer, Phys. Rev. Lett. 34 (1975) 43 and Phys. Rev. D12 (1975) 1404.
- [2] S.J. Brodsky, T.A. DeGrand, R.R. Horgan and D.G. Coyne, Phys. Lett. B73 (1978) 203;  
K. Koller, T. Walsh, Nucl. Phys. B140 (1978) 449.
- [3] S.J. Brodsky, G.F. Lepage and P.B. Mackenzie, Phys. Rev. D28 (1983) 228.
- [4] A. Ore and J.L. Fowell, Phys. Rev. 75 (1949) 1696.
- [5] D.M. Photiadis, Phys. Lett. B164 (1985) 160.
- [6] R.D. Field, Phys. Lett. B 133 (1983) 248.
- [7] Crystal Ball Collab., K. Wachs et al., Zeit. Phys. C42 (1989) 33;  
Crystal Ball Collab., D.A. Williams et al., Phys. Rev. D 38 (1988) 1365;  
E.D. Bloom, C.W. Peck, Ann. Rev. Nucl. Part. Sci. 33 (1983) 143.
- [8] B. Andersson et al., Phys. Rep. 97 (1983) 31;  
T. Sjöstrand, Comp. Phys. Comm. 39 (1986) 347.
- [9] R. Ford and W. Nelson, SLAC-210 (1978), unpublished.
- [10] H. Fesefeld, PITHA 85/02, unpublished.
- [11] ARGUS Collab., H. Albrecht et al., Phys. Lett. B199 (1987) 291.
- [12] CLEO Collab., S.E. Csorna et al., Phys. Rev. Lett. 56 (1986) 1222.
- [13] CUSB Collab., R.D. Schamberger et al., Phys. Lett. B138 (1984) 225.
- [14] J. Schütte, Ph.D. thesis, Universität Erlangen-Nürnberg (1989),  
DESY F31-89-03, unpublished.
- [15] Crystal Ball Collab., P. Schmitt et al., Zeit. Phys. C40 (1986) 199.
- [16] A. Bizzeti, Ph.D. thesis, Università di Firenze (1987), unpublished.
- [17] F.A. Berends, R. Kleiss, Nucl. Phys. B228 (1983) 537.
- [18] TASSO Collab., W. Braunschweig et al., Zeit. Phys. C41 (1988) 385.
- [19] D.W. Duke and R.G. Roberts, Phys. Rep. 120 (1985) 227.
- [20] R. Marshall, Proc. XXIV Int. Conf. on High Energy Physics (Munich, 1988), eds.  
R. Kotthaus and J.H. Kühn (Springer-Verlag, Berlin, Heidelberg, 1988) p. 901.

## Figure Captions

Figure 1: The on-resonance energy spectrum of photon candidates (solid histogram), together with the scaled continuum spectrum (dotted histogram). The  $\pi^0$  spectrum is shown as solid points and is fitted with an exponential shape (solid curve), see the section on *Statistical Analysis of Shower Shape*.

Figure 2: The total efficiency for the detection of direct photons from the decay  $\Upsilon(1S) \rightarrow \gamma\gamma\gamma$ . This efficiency applies to the analysis according to method 1 (*Statistical Analysis*); for method 2 this efficiency is reduced by about 40% due to harder cuts on the lateral shape of photon showers.

Figure 3: An example of a simultaneous fit of the  $\Theta^2$  distribution of photons (dashed line) and  $\pi^0$ 's (dotted line) to the  $\Theta^2$  distribution of the photon candidates with  $0.6 < z < 0.65$  (crosses). The solid line is the sum of the two fitted distributions.

Figure 4: The direct photon spectrum after efficiency correction obtained by subtracting the on-resonance background using the  $\Theta^2$  fitting procedure described in the text (method 1). The data are fitted to Field's model [6] (solid line), to Photiadis' model [5] (dotted line) and to the lowest order QCD prediction [2] (dashed line).

Figure 5: The direct photon spectrum after efficiency correction obtained by subtracting the on-resonance background using a Monte Carlo simulation of the background (method 2). The data are fitted to Field's model [6] (solid line), to Photiadis' model [5] (dotted line) and to the lowest order QCD prediction [2] (dashed line).

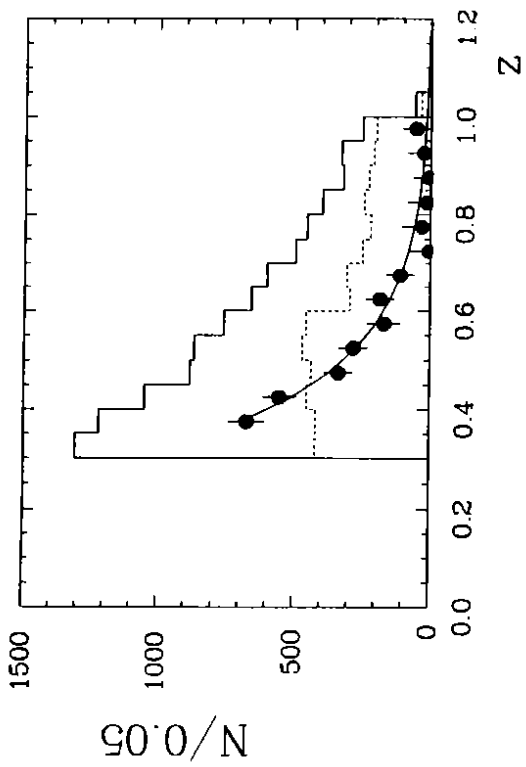


Fig. 1

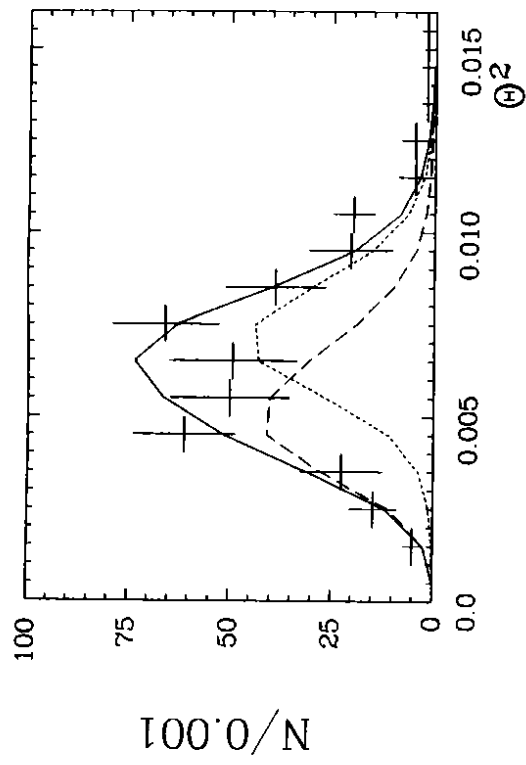


Fig. 3

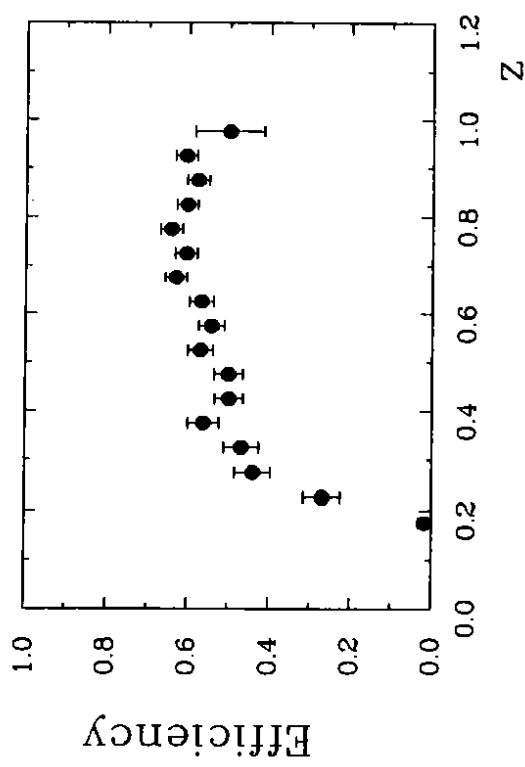


Fig. 2

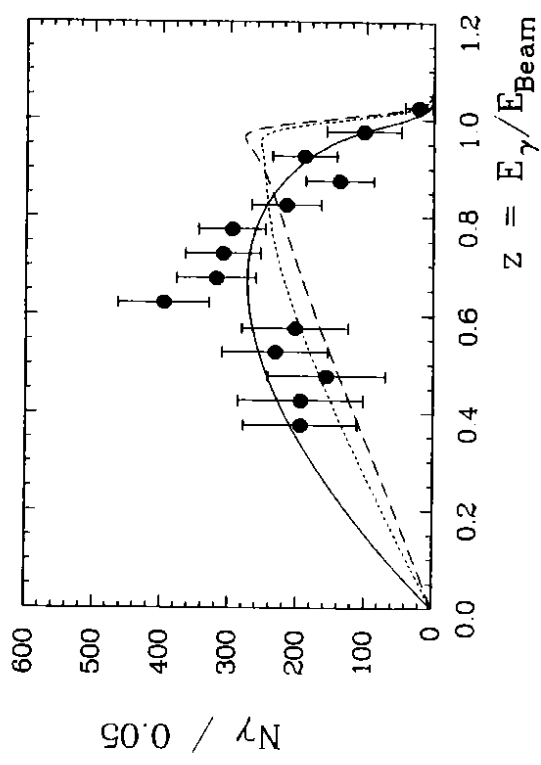


Fig. 4

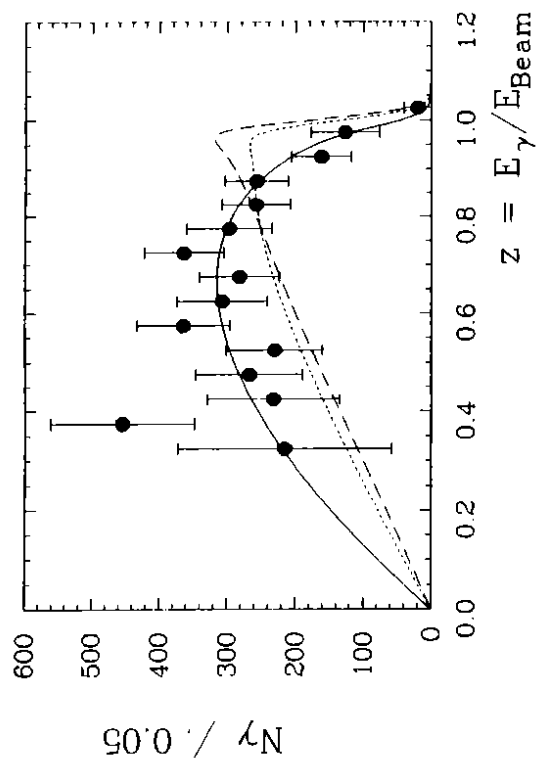


Fig. 5